remote sensing

MDPI

Article

Footprint of the 2020 COVID-19 Lockdown on Column-Integrated Aerosol Parameters in Spain

María Ángeles Obregón *, Blanca Martín and Antonio Serrano

Departamento de Física, Instituto del Agua, Cambio Climático y Sostenibilidad, Facultad de Ciencias, Universidad de Extremadura, 06006 Badajoz, Spain; asp@unex.es (A.S.)
* Correspondence: nines@unex.es

Abstract: The lockdown adopted in Spain to combat the global pandemic due to the coronavirus disease (COVID-19) led to a significant reduction in the emission of aerosols produced by road traffic and industry. This study aims to detect changes in column aerosols in Spain due to the COVID-19 lockdown. High-quality AErosol RObotic NETwork (AERONET) measurements of AOD (aerosol optical depth), AE (Ångström exponent) and SSA (single scattering albedo) over the period 2012–2020 are used for this purpose. Ten AERONET stations with available measurements during the lockdown and post-lockdown periods with a long previous data record are selected. The stations are well distributed throughout Spain, covering different areas and population densities. A comprehensive set of three statistical tests are applied to assess general changes in the dataset, the central tendency and low and high values for each parameter. The analyses are conducted for the 2020 lockdown and post-lockdown periods by comparing daily aerosol data with the measurements recorded for the same calendar days during the period 2012–2019. The results indicate a general increase in AOD during the lockdown and a decrease during the post-lockdown. While AE shows no overall behaviour, SSA is the parameter most sensitive to changes in anthropogenic contribution, with an overall significant increase in almost all the stations during both lockdown and post-lockdown periods. The study contributes to addressing the impact of the COVID-19 lockdown and provides methodologies to detect its footprint.

Keywords: COVID-19; lockdown; column aerosol; AERONET; Spain

Citation: Obregón, M.Á.; Martín, B.; Serrano, A. Footprint of the 2020 COVID-19 Lockdown on Column-Integrated Aerosol Parameters in Spain. *Remote Sens.* **2023**, *15*, 3167. https://doi.org/10.3390/rs15123167

Academic Editor: Alexander Kokhanovsky

Received: 12 May 2023
Revised: 14 June 2023
Accepted: 15 June 2023
Published: 18 June 2023

1. Introduction

The sudden outbreak of the 2019 coronavirus disease (COVID-19) began in Wuhan, China, in December 2019, and has since spread around the world, resulting in more than 764 million confirmed cases and almost 7 million deaths according to the World Health Organisation (https://covid19.who.int/, accessed on 5 March 2023). To control the rapid spread of the disease, many countries took drastic measures to restrict human mobility, which led to a sharp decrease in human activities and, subsequently, to significant reductions in gas and aerosol emissions. In particular, this situation led to a significant cut in the emission of aerosols produced by road traffic and industry.

This unexpected situation provides unique conditions to study the human contribution to the total aerosol load since, in this period, the anthropogenic component was notably reduced and the aerosol load was almost exclusively due to natural sources. The discrimination between anthropogenic and natural origins of aerosols is a scientific issue of utmost importance since aerosols play a key role in climate change [1,2]. Indeed, uncertainties in understanding the effects of aerosols in altering the radiative balance of the Earth-atmosphere system and the hydrological cycle are currently a major limitation to our understanding of climate change [3]. In addition to affecting climate, aerosol loading degrades the ground-level air quality and causes detrimental effects on human health.

Taking advantage of this unusual situation, several studies have been conducted around the world at different spatial scales. Many of them focus on PM2.5 and PM10 (particles smaller than 2.5 and 10 microns, respectively) in situ measurements registered near the ground and their effect on air quality, and others use radiometric measurements to study the entire aerosol column.

Some studies have addressed the effect of the pandemic on a global scale by analysing air quality during the COVID-19 lockdowns in several selected cities around the world [4,5]. Their results indicate a substantial reduction in primary air pollutants [6,7] and, specifically, an overall reduction in PM2.5 in the most polluted capital cities of the world [7–9]. The effect on the column aerosol has also been observed at the global scale by several satellites such as MODIS and CALIOP, with wide areas of the world being covered [10–13].

Specifically, a large number of studies have been conducted in Asia, primarily in China, as this is where the first COVID-19 cases were detected. Thus, an improvement in air quality due to the severe two-month lockdown imposed was reported for Wuhan [14], the Chinese city where the new coronavirus emerged. A decrease in particulate matter (PM) was also found in other Chinese megacities, such as Xi'an [15] and Shanghai [16], which often face air pollution problems. This change also affected the formation of secondary particulate matter. Thus, the sharp decrease in NO_x emissions from road traffic increased the formation of ozone and nocturnal NO_3 radicals, and this increase in atmospheric oxidation capacity, in turn, favoured the formation of secondary pollution [17]. The restriction on using private vehicles notably contributed to the reduction in PM2.5 and PM10 in many Chinese cities [18]. However, in contrast to southern and central China, PM2.5 increased substantially in northern China, with some severe haze events occurring in Beijing during the three weeks of the lockdown [19]. This dissimilar behaviour reveals the spatial variability of the contribution of natural and anthropogenic sources of aerosols and the need for local studies in different areas.

A general reduction in aerosols also occurred in other highly populated Asian cities such as Delhi in India [20], Almaty in Kazakhstan [21], Tokyo in Japan [22], Jakarta in Indonesia [23] and Bangkok in Thailand [24], for example.

In addition to air quality studies, a few studies have investigated the effect of lockdowns on the column aerosol in Asia. Thus, Shukla et al. [25] analysed measurements from the AErosol RObotic NETwork (AERONET) station at Kanpur (India) and reported decreases in the aerosol optical depth (AOD) and Ångström exponent (AE). On the other hand, Shen et al. [26] studied the column aerosol in the Chinese province of Hubei using MODIS satellite data, finding a general decrease in AOD and an increase in AE. The opposite sign of the variation in AE between Kanpur (India) and Wuhan (China) highlights the interest to conduct local studies, in order to account for the high variability of aerosol sources.

The impact of the COVID-19 lockdown on air quality has also been monitored in other regions around the world: North America [27,28], Central America [29], South America [30–32] and Australia [33], for example.

Several other studies have focused on the effects of the COVID-19 restrictions on air quality in European countries such as Sweden [34], United Kingdom [35], Germany [36], Poland [37], Italy [38], France [39–42] and Portugal [43,44]. A reduction in PM2.5 of 40% in Sweden, the United Kingdom, France and Spain was reported in [34]. The largest reductions in PM2.5 occurred at urban traffic sites, being more modest at background locations where a large proportion of the population lives [35].

Regarding the studies of column aerosol, the AERONET measurements showed that, while AOD decreased in Italy [45] during the lockdown, it increased in France [46]. These measurements were in line with MODIS satellite measurements, which observed a significant reduction in AOD in Poland [47] and most areas in Europe, except for its western part, where it increased [10,11]. The study of Sannino et al. [48] in Italy is of particular interest since they found that the AOD for the entire aerosol column increased in contrast to the PM10 measured near the ground, which decreased. The opposite behaviour

between the aerosol near the ground and the entire aerosol column reported by this study emphasises the need for studying both types of measurements.

Within Europe, the Iberian Peninsula is an area of particular interest due to its location, as it is affected by a large variety of natural and anthropogenic sources of aerosols. Thus, it is influenced by maritime air masses coming from the Atlantic Ocean or the Mediterranean Sea, along with continental air masses coming from Europe, and dust intrusions originating in the south, in the Sahara Desert. Therefore, several studies have also been conducted on the effects of the restrictions in this area. Most of them have focused on air quality in densely populated cities such as Barcelona [49], Madrid [50] or Valencia [51], in selected groups of cities [41,42] or in extensive networks with a large number of stations covering both urban and rural areas [52]. In general terms, all these in situ studies have reported a reduction in the PM recorded at ground level.

However, little research has been conducted on the effect of the lockdown on column aerosol measurements. In fact, apart from some above-mentioned global studies using satellite data, to our knowledge, only Barragán et al. [53] analysed the column aerosol over Spain using radiometric measurements from surface stations, despite the fact that the AERONET network offers high-quality long-term data at different temporal resolutions (from day to months) at many locations. The study of Barragán et al. [53], although innovative and interesting, is limited to one location: Madrid. Therefore, a broader study covering several areas is necessary to achieve general conclusions on the national scale.

In this context, the present study is conducted to detect the footprint of the 2020 COVID-19 lockdown on column-integrated aerosol parameters in several locations in Spain. This area was selected since it was all constrained by the same restrictions, which were prompted by scientific experts [54]. For this purpose, high-quality aerosol data from ten stations belonging to the AERONET global network were selected. The locations are spatially distributed over peninsular Spain so as to have a dataset representative of the area of study. The period of study covers 2012 to 2020, guaranteeing sufficient temporal representativity. The values of the three column-integrated aerosol parameters most commonly used in aerosol studies (AOD, AE and single scattering albedo (SSA)) during the lockdown and post-lockdown periods are compared with typical values measured for the same calendar months in previous years, and the significance of the differences is addressed.

The paper is organised as follows: Section 1 introduces the topic and goals of the study, Section 2 describes the instrumentation and dataset, Section 3 presents the methodology, Section 4 shows the results obtained, Section 5 discusses the results in a combined view and Section 6 draws some conclusions.

2. Instrumentation and Data

This study relies on radiometric measurements of atmospheric aerosol made with CIMEL CE-318 sunphotometers integrated into the NASA AERONET network [55]. The CIMEL CE-318 sunphotometer measures direct sun irradiances and sky radiances at several wavelengths between 340 and 1020 nm. For more details on this instrument, see Holben et al. [55]. All measurements are processed according to the AERONET protocols described by Holben et al. [55], obtaining aerosol parameters at different quality levels: Level 1.0 (unscreened), level 1.5 (cloud-screened and quality-controlled), and level 2.0 (quality-assured).

In order to achieve a thorough characterization of the aerosol, the three parameters most commonly used in aerosol studies have been analysed: the AOD at 440 nm, the AE retrieved using the wavelengths 440, 500, 675 and 870 nm and the SSA at 440 nm. These parameters give key information about the different radiative properties of the aerosol. Thus, while AOD is a measure of the total attenuation suffered by the solar radiation due to the aerosol load, AE is related to the size of aerosol particles, and SSA measures the proportion of the radiation attenuated by aerosol that is due to scattering, in contrast to that due to absorption.

The AERONET protocols guarantee the high quality of its data. Thus, the uncertainty in the AOD as estimated by Holben et al. [55] is 0.01 for wavelengths longer than 440 nm

and 0.02 for wavelengths shorter, with 0–0.5 being the typical range of AOD values. This uncertainty leads to a deviation of 0.03–0.04 in the AE [56], whose typical values lie between 0 and 2.5. According to Dubovik et al. [57], the SSA uncertainty is 0.03 for water-soluble aerosols when AOD440 is above 0.2, and also 0.03 for dust and biomass burning when AOD440 is above 0.5. This uncertainty increases to 0.05–0.07 when AOD440 is below 0.2 for AOD440 $\leq$ 0.2. Since SSA typically ranges between 0.5 and 1, its uncertainty is generally approximately 6–7% of the value.

Daily level 1.5 data have been used in this study due to the very low number of SSA data at level 2.0. The main reason for this scarcity is the condition to only include cases with AOD at 440 nm greater than 0.4. These AOD values are very uncommon in peninsular Spain and correspond almost exclusively to desert dust intrusions. Therefore, level 1.5 represents an interesting choice that combines quality and availability of measurements.

The area of study covers peninsular Spain, where many AERONET stations provide long-term series of high-quality measurements. Several stations must be considered if conclusions at a national scale are to be drawn since they are affected by a large variety of aerosol sources. Thus, Spain is located in southwestern Europe and in close proximity to North Africa. The main natural aerosol sources are maritime air masses coming from the Atlantic Ocean and the Mediterranean Sea, polar air masses and air masses coming from the Sahara Desert. The Sahara Desert is an important source of mineral aerosols in the Northern Hemisphere and especially over Spain, due to the proximity between these two regions and the annual latitudinal shift of the general atmospheric circulation, which shows a marked seasonal pattern. In addition to these large-scale contributions, local aerosol sources must be considered. The anthropogenic contribution in Spain is diverse, with densely populated and industrialised cities such as Madrid and Barcelona, and other rural areas where activities focus more on agriculture and livestock.

The period of study was chosen, taking into account the restrictions established by the Spanish government. Specifically, the lockdown of the population began on 14 March 2020 and ended in most regions (administratively named "autonomous communities") on 11 May 2020. During this period, the same restrictions applied to the whole country, so it can be assumed that the aerosol measurements at different locations were affected similarly. This period has been called the "lockdown period". On 11 May 2020, the de-escalation phase began, and each region established its own restrictions. Therefore, it is interesting to analyse the site-specific conditions of each station. This period is interesting since it is affected by the long-term effect of the restrictions imposed during the lockdown. This second period is called the "post-lockdown period" and runs until 31 July 2020.

As mentioned above, the study focuses on Spain to guarantee that all selected locations were subject to the same restrictions. Two requirements were adopted for the selection of the stations to study: (1) the availability of data for the COVID-19 lockdown and post-lockdown periods in 2020, and (2) a minimum number of years prior to the pandemic to ensure the statistical significance of the study. Fifteen AERONET stations fulfilled the first criterion, i.e., they had been registering measurements during the lockdown and post-lockdown periods. However, the number of years with data differs greatly from location to location. Figure 1 shows the number of stations with available data per year. In 2012, stations increased from seven to twelve, therefore the period of 2012–2020 was chosen as a compromise between the stations and the number of records. These stations are located at El Arenosillo, Badajoz, Barcelona, Burjassot, A Coruña, Granada, Madrid, Montsec, Murcia, Palencia, Valladolid and Zaragoza. Finally, two of these stations, El Arenosillo and Montsec, were excluded because their number of measurements in the calendar months of interest (March–July) was very low.

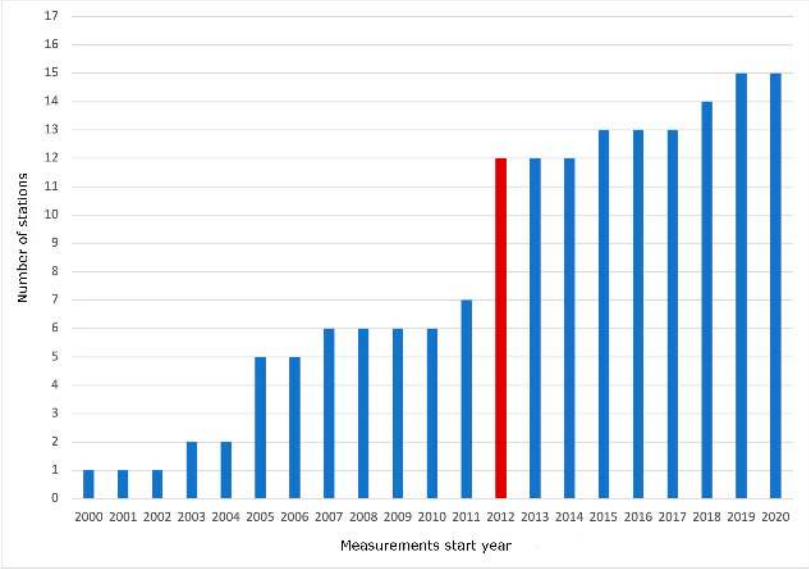

Figure 1. Stations with available data per year. The final selection is coloured in red.

The ten final selected stations are well-distributed throughout peninsular Spain (Figure 2). These stations are representative of the different aerosol contributions that affect Spain and can be grouped according to different criteria. For example, while some are located within large cities and are affected by a highly urban environment, such as Madrid and Barcelona, others are more rural, such as Badajoz and Palencia. Regarding the influence of the two large bodies of water surrounding the Iberian Peninsula, the Atlantic Ocean and the Mediterranean Sea, the stations can be broadly divided into three groups: (1) Atlantic stations, such as A Coruña, Badajoz, Valladolid and Palencia; (2) Mediterranean stations, such as Murcia, Burjassot and Barcelona; and (3) those stations located in the middle, such as Granada, Madrid and Zaragoza, with a double Atlantic and Mediterranean influence and notably influenced by the orography of their surroundings. Another important aspect to take into account is the proximity to the sea. Thus, the sea–land breeze plays a key role in air renewal in coastal stations such as A Coruña, Barcelona, Burjassot and Murcia. In addition to maritime air masses, Spain is frequently affected by dust intrusions from the Sahara Desert, which is the main source of mineral aerosols in the northern hemisphere. These intrusions are common in southern stations such as Granada, Badajoz, Murcia and Burjassot, being less frequent as latitude increases.

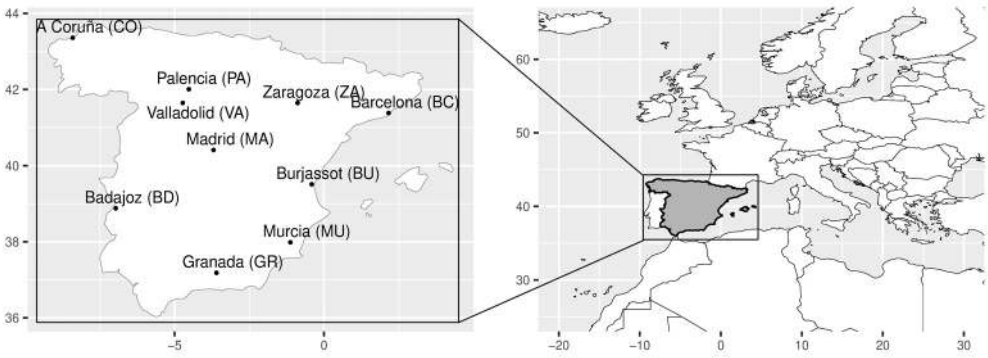

Figure 2. Locations, names and abbreviations of the AERONET stations used in the study.

On the other hand, the eight years of measurements guarantee the temporal significance of the data and favour the reliability of the conclusions. It is important to note the large variability shown by the column aerosol in peninsular Spain, due to the effect of

different sources of various spatial scales. Thus, the ten selected stations are a good choice that combines a high number of stations and a large number of records.

3. Methodology

Once the period of study and the stations were selected, the corresponding time series were analysed. The analysis relied on three different statistical tests focusing on distinct aspects of the probability distribution of the data. It must be acknowledged that the use of inference tests based on *p*-values is controversial since they can result in false positives too often [58]. However, there is no general consensus on the alternative method to be used [59] since they are limited to visual analysis or involve subjective assumptions that could bias the results [60]. Therefore, *p*-values are presently widely accepted and used in this field. In our study, in order to minimise the possible effect of too often false positives, several statistical analyses focusing on distinct aspects of the probability distribution of the data were performed, and the final conclusions are derived from the combined view of all the results.

Firstly, a global analysis of all stations consisting of a two-factor ANOVA (ANalysis Of VAriance) test [61,62] was used to check the effect of the location and the period on the data. Secondly, a central tendency test was applied to detect differences in the median. Lastly, the behaviour of the lower and upper tails of the probability distribution was analysed by means of a proportion hypothesis test. The aim of the analyses is to detect changes in data in the lockdown and post-lockdown periods in 2020 compared to the previous 2012–2019 time series, which acts as the reference. While the first analysis is applied jointly to all stations, the second and third tests are applied individually to each station.

3.1. General Analysis (First Statistical Test)

The first study consisted of a global analysis including all stations at once. The analysis was an ANOVA test with two factors: the location and the period. Two tests were performed: one compared the lockdown period with the reference period 2012–2019, and the other compared the post-lockdown period with the same reference period.

This test was developed by R. A. Fisher in 1930 and analyses the possible effects of one or more factors over a variable based on the decomposition of the variance of a sample of data. Thus, it allows us to determine whether there is a statistically significant difference between the means of the aerosol parameters grouped by the location and by the period. The ANOVA model assumes that:

$$x_{ij} = \mu + \alpha_i + \beta_j + \cup, \tag{1}$$

With x_{ij} being each aerosol parameter (AOD, AE or SSA) value corresponding to the i-th value of the factor Y (location, with i = 10 levels) and to the j-th value of the factor Z (period, with j = 2 levels: period of study and reference period). The variable μ represents the mean of all data, α_i is the effect of the i-th level of the factor Y ($i \in 1, \ldots, I$), β_j is the effect of the j-th level of the factor Z ($j \in 1, \ldots, J$) and U represents the variability of the variable X. By definition, the sum of the effects of each factor always equals zero, i.e., $\sum_{i=1}^{I} \alpha_i = 0$ and $\sum_{j=1}^{J} \beta_j = 0$. In the case that the factor Y, for example, has no influence on the variable X, then each α_i equals zero. The same applies to factor Z.

The ANOVA test is based on the decomposition of the variance of the variable X, as follows:

$$\sum_{i=1}^{I}\sum_{j=1}^{J}\left(x_{ij} - \overline{x}_{..}\right)^2 = J\sum_{i=1}^{I}\left(\overline{x}_{i\,.} - \overline{x}_{..}\right)^2 + I\sum_{j=1}^{J}\left(\overline{x}_{.\,j} - x_{..}\right)^2 + \sum_{i=1}^{I}\sum_{j=1}^{J}\left(x_{ij} - \overline{x}_{i\,.} - \overline{x}_{.\,j} + \overline{x}_{..}\right)^2, \tag{2}$$

With $\overline{x}_{..}$ being the mean of all x_{ij} data, $\overline{x}_{i\,.}$ being the mean of the data with i-th level of factor Y and any level of factor Z and $\overline{x}_{.j}$ being the mean of the data with any level of factor

Y and *j*-th level of factor Z. Thus, the left side of Equation (2) represents the total sum of squares (SCT); the first summand of the right side of the equation is the sum of squares explained by factor Y (SCE(α)), the second summand is the sum of squares explained by factor Z (SCE(β)) and the third summand is the residual sum of squares (SCR).

The test compares the sum of squares explained by one factor with the residual sum of squares. For that aim, the following statistic is built for factor Y:

$$F_\alpha = \frac{\frac{SCE(\alpha)}{I-1}}{\frac{SCR}{(I-1)(J-1)}}. \quad (3)$$

The test is applied with the null hypothesis of no influence by factor Y, i.e., $\alpha_1 = \alpha_2 = \ldots = \alpha_J = 0$. The statistic F_α is calculated, and if its *p*-value is lower than 0.05 the null hypothesis is rejected, concluding that there is a significant influence of the factor Y on the variable X. The test is applied similarly for the factor Z.

Although the ANOVA test is based on the assumptions of normal populations and equal group sample size, several studies have provided empirical evidence for the robustness of *F*-test even when normality is violated (for example, [63–65]). Additionally, the Monte Carlo method has also been used to test how ANOVA behaves with non-normal data and unequal group sample sizes, finding it could be still considered a valid option [66]. In this study, the ANOVA test has been applied as the first analysis. It is followed by individual analyses for each location and the final conclusions will be based on the combined view of all results.

3.2. Central Tendency Analysis (Second Statistical Test)

This test is applied to determine whether there have been statistically significant changes in the median of the aerosol parameters due to COVID-19. The test was applied to each station comparing the lockdown and post-lockdown periods with the reference period of 2012–2019. For that aim, the *t*-test or Mann–Whitney–Wilcoxon's test can be used provided their requirements are fulfilled. While the *t*-test requires the data to follow a normal distribution, Mann–Whitney–Wilcoxon's test has no requirements on the probability distribution followed by the data. Thus, the first step was to test the 2012–2019 time series of the three aerosol parameters at the ten selected stations for normal distribution using Shapiro–Wilks' test (1965). All the time series resulted in being non-normal at 95% confidence and, therefore, the non-parametric Mann–Whitney–Wilcoxon's test was chosen.

This test compares the median of two probability distributions. It is based on the statistic *U* built from two samples of X of size *n*: $x_1, x_2, \ldots, x_n$, and Y of size m: $y_1, y_2, \ldots, y_m$, as follows:

$$U = \sum_{i=1}^{n} \sum_{j=1}^{m} S(x_i, y_j), \quad (4)$$

where *S(X,Y)* is defined as:

$$S(X, Y) = \begin{Bmatrix} 1\ if\ X > Y \\ \frac{1}{2}\ if\ X = Y \\ 0\ if\ X < Y \end{Bmatrix}. \quad (5)$$

For samples as large (equal o larger than 20) as ours, statistic z follows a normal distribution N (0,1):

$$z = \frac{U - \frac{nm}{2}}{\sqrt{\frac{nm(n+m+1)}{12}}}. \quad (6)$$

The value of *z* is calculated, and if its *p*-value is lower than 0.05 the null hypothesis is rejected, concluding that the median has significantly changed from 2012–2019 to 2020. The test was applied to the three aerosol parameters at the ten selected locations for both periods: lockdown and post-lockdown.

3.3. Proportions Hypothesis Test (Third Statistical Test)

This test analyses the lower and upper tails of a probability distribution. It aims to detect changes in the extreme values of the aerosol parameters measured in 2020 compared to the 2012–2019 period. In this study, the first, Q1 (percentile 25), and third, Q3 (percentile 75) quartiles of the distribution are chosen to represent the lower and upper tails, respectively.

For that test, a dichotomous variable is defined, which equals 1 if a value is lower (or higher) than the Q1 (or Q3) and equals 0 otherwise. In order to compare two sets of data X and Y (in our case, 2012–2019 and 2020 time series), two discrete Bernoulli's probability distributions are used with the probability of success p_x and p_y, respectively, which are also the corresponding means of the probability distributions. The null hypothesis of the test is that the proportions of the two populations are equal, that is, $p_x = p_y$. They are set to 0.25 when testing low values and 0.75 when testing high values. For samples with more than 20 data (as in our study), the probability distribution of the mean of the sample approaches a normal distribution and a z-test can be used.

With $\hat{p}_x$ and $\hat{p}_y$ being the sample proportions and n and m the size of the data X and Y, respectively, the statistic z can be built as follows:

$$z = \frac{\hat{p}_x - \hat{p}_{y2}}{\sqrt{\frac{p_x(1-p_x)}{n} + \frac{p_y(1-p_y)}{m}}}; \quad (7)$$

which, under the hypothesis of equal proportions, follows a normal distribution N (0,1). The first (or third) quartile Q1 (Q3) is calculated from the 2012–2019 reference data set and the sample proportion of the values of the 2020 dataset, which are lower (higher) than that Q1 (Q3) is obtained. This calculation is performed for each aerosol parameter, each location, lower and upper thresholds and lockdown and post-lockdown periods. Then, z is calculated, and if its corresponding p-value is lower than 0.05, the existence of a significant difference in proportions between the two populations can be concluded.

4. Results

4.1. Preliminary Analysis

In order to have reference values to compare the lockdown and post-lockdown values with, the daily values of the aerosol parameters during the period 2012–2019 for each calendar day were averaged. The mean value and the 95% percentile interval for each calendar day are plotted in Figures 3–5 in black and light blue colours, respectively. Superimposed to these lines, the daily values registered during the 2020 lockdown and post-lockdown are plotted in red and yellow, respectively. A notable variability is observed in all three aerosol parameters, as a result of the alternation of distinct aerosol contributions driven by different synoptic circulations.

It can be observed that, during the lockdown period, the AOD values are generally within the confidence interval, although stations such as Barcelona, Burjassot, Murcia and Zaragoza show episodes with values notably higher. In contrast, during the post-lockdown period, there seems to be a general tendency for the values to be somewhat lower than the reference.

With respect to AE, no predominant general pattern is observed in most stations during the lockdown and post-lockdown periods (Figure 4). A notable scatter around the reference values is shown, with a few extreme values in each location.

Figure 5 illustrates the mean annual evolution of the SSA values for the reference period, along with the values registered during the 2020 lockdown and post-lockdown periods. A clear pattern can be observed for this parameter, with values being higher than the reference for most stations during both lockdown and post-lockdown periods. Only Palencia station clearly deviates from this general behaviour.

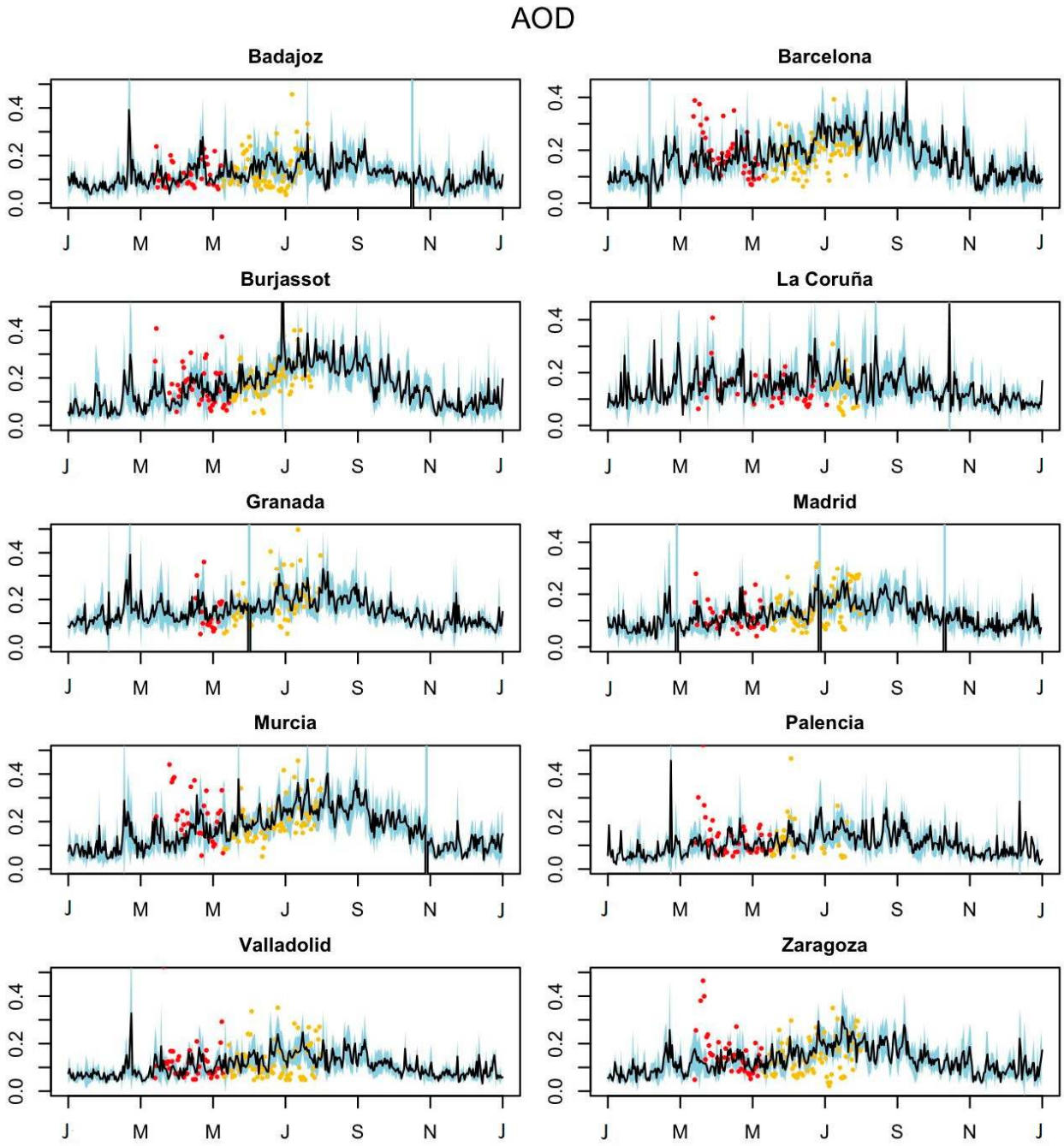

Figure 3. Evolution of AOD throughout the year for each selected location: mean daily values for the reference period 2012–2019 (in black), their 95% percentile interval (in light blue), 2020 lockdown values (in red) and 2020 post-lockdown values (in yellow). The x-axis shows the date (J = January; M = March; M = May; J = July; S = September; N = November).

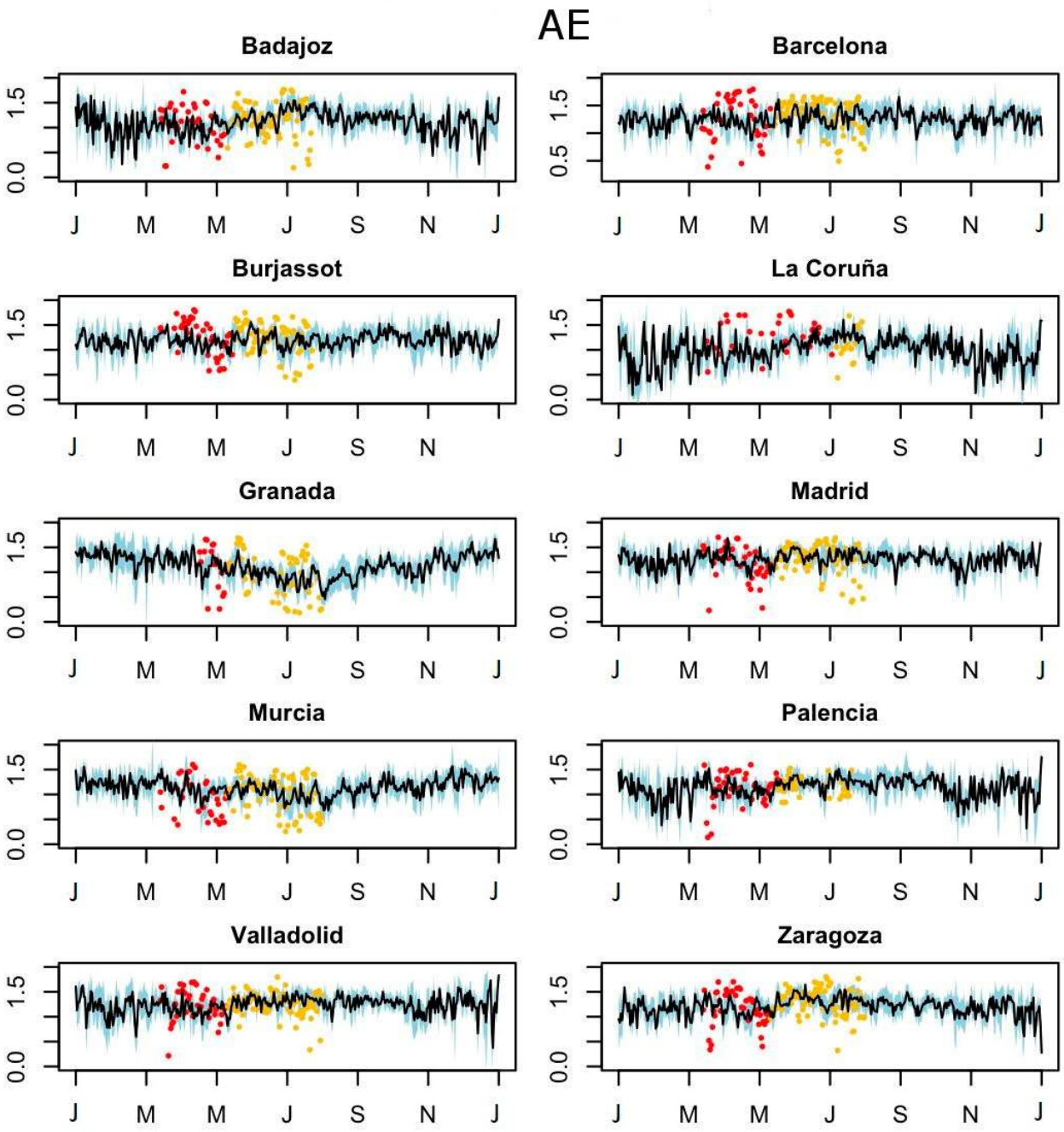

Figure 4. Evolution of AE throughout the year for each selected location: mean daily values for the reference period 2012–2019 (in black), their 95% percentile interval (in light blue), 2020 lockdown values (in red) and 2020 post-lockdown values (in yellow). The x-axis shows the date (J = January; M = March; M = May; J = July; S = September; N = November).

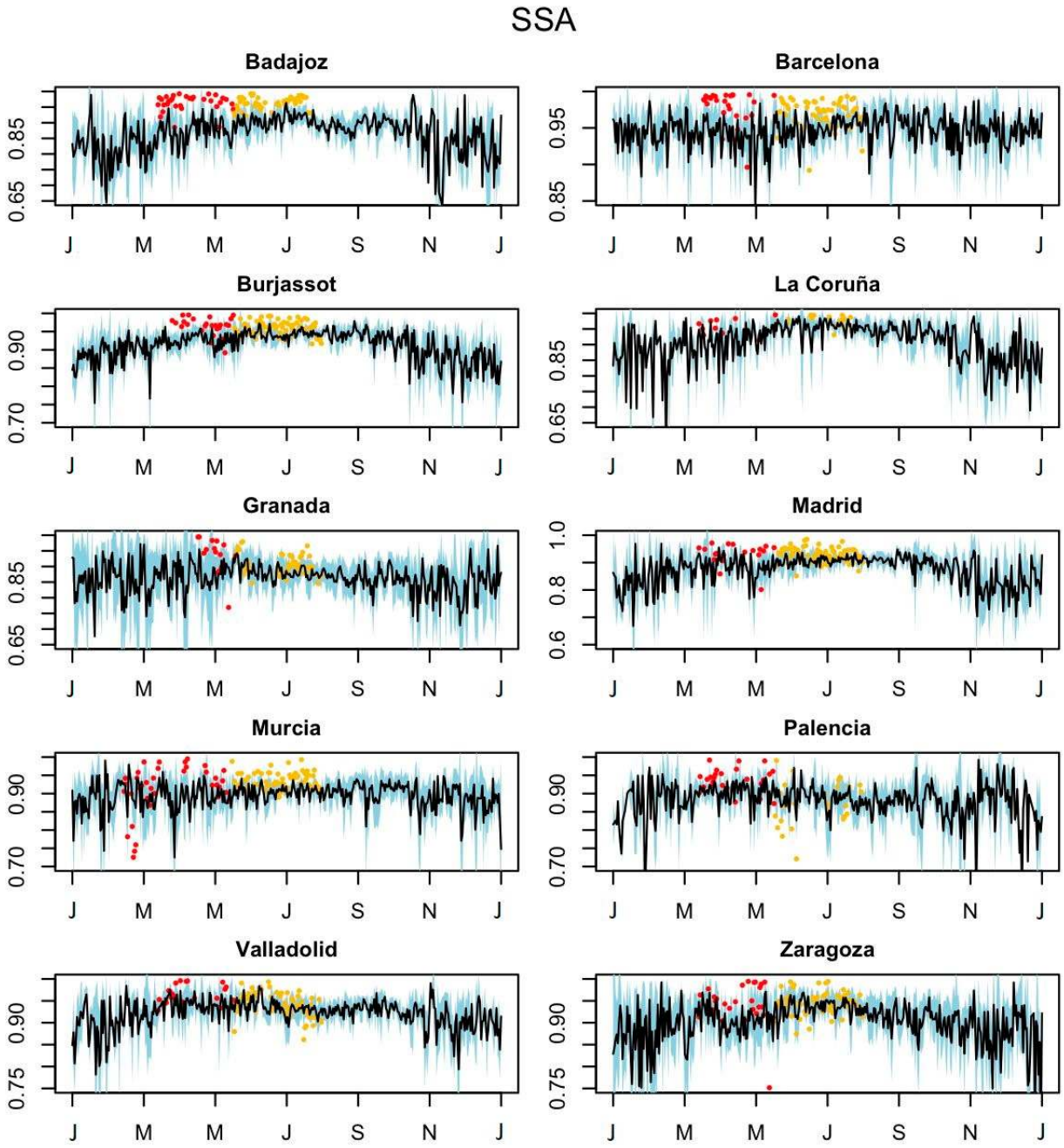

Figure 5. Evolution of SSA throughout the year for each selected location: mean daily values for the reference period 2012–2019 (in black), their 95% percentile interval (in light blue), 2020 lockdown values (in red) and 2020 post-lockdown values (in yellow). The x-axis shows the date (J = January; M = March; M = May; J = July; S = September; N = November).

4.2. General Analysis

This analysis examines whether the values of aerosol parameters have changed in general terms, i.e., considering the ten stations simultaneously. For this purpose, the ANOVA test with two factors (location and time) was applied. Two ANOVA tests were performed: One compared the 2020 lockdown period with the same calendar days of the years 2012–2019, and the other compared the 2020 post-lockdown period with the same calendar days of the years 2012–2019. The results of applying these tests to each of the three studied aerosol parameters are presented in Table 1. These results show that AOD and SSA differ significantly as a function of both "time" and "location" factors. This means that

AOD and SSA during the lockdown and post-lockdown differ from the values registered during the same calendar days during the period 2012–2019. Regarding AE, there is no significant evidence of general change between the time periods. However, significant AE differences are found for the "location" factor, suggesting an analysis of each location individually. The ANOVA test is also significant for SSA with both factors "location" and "time", confirming what was observed in the preliminary analysis.

Table 1. Results of the ANOVA test for AOD, AE and SSA during the lockdown and post-lockdown periods. *p*-values < 0.05 are shown in bold. The text "$<2 \times 10^{-16}$" indicates that the number obtained in the test is lower than 2×10^{-16}, which is the computer precision.

	AOD		**AE**		**SSA**	
	Location	**Time**	**Location**	**Time**	**Location**	**Time**
	***p*-Value**		***p*-Value**		***p*-Value**	
Lockdown	$\mathbf{<2 \times 10^{-16}}$	$\mathbf{3.83 \times 10^{-7}}$	$\mathbf{<2 \times 10^{-16}}$	0.271	$\mathbf{<2 \times 10^{-16}}$	$\mathbf{<2 \times 10^{-16}}$
Post-lockdown	$\mathbf{<2 \times 10^{-16}}$	$\mathbf{6.67 \times 10^{-6}}$	$\mathbf{<2 \times 10^{-16}}$	0.141	$\mathbf{<2 \times 10^{-16}}$	$\mathbf{<2 \times 10^{-16}}$

It is important to mention that the ANOVA test has been shown to be significant for the "location" factor in all three aerosol parameters. This fact indicates the need to perform a more thorough study with each location being analysed individually. Since the ANOVA analysis performs a global examination, there may be differences at specific stations that could be masked when all stations are considered together.

4.3. Central Tendency Analysis

After the global analysis, the next step was to determine whether there were significant changes in the median between the 2020 lockdown and post-lockdown periods, and the reference period 2012–2019. For this purpose, Mann–Whitney–Wilcoxon's test was applied, and the results are shown in Figure 6.

These results indicate that the median of the AOD during the 2020 lockdown period was significantly higher than the median of the AOD reference values at six stations out of the ten of the study: Barcelona, Burjassot, Murcia, Palencia, Valladolid and Zaragoza. These AOD variations can be observed in Figure 7a, where the boxplots allow the distributions to be compared. This behaviour reversed during the 2020 post-lockdown period, when the median AOD was significantly lower than the median of the reference values at Barcelona, Burjassot, A Coruña and Zaragoza (Figure 7b). It is important to mention that the three eastern stations (Barcelona, Burjassot and Zaragoza) showed significant deviations compared to the reference values, being higher during the lockdown and lower during the post-lockdown period.

Regarding AE, less-clear results are obtained, since only two stations (Murcia and A Coruña) show significant changes in the median between the 2020 lockdown values and the 2012–2019 reference values (Figure 6c), and the sign of their variation differs: a decrease at Murcia and an increase at A Coruña (Figure 8a). In the 2020 post-lockdown period, three western stations (Badajoz, Palencia and Valladolid) showed a significant decrease compared to the reference values (Figures 6d and 8b).

The clearest general behaviour is found in the SSA values, with all ten stations showing a significant increase in the 2020 lockdown period (Figure 6e) compared to the reference values and six out of ten in the 2020 post-lockdown period (Figure 6f). This increase in SSA can be clearly observed in Figure 9. It indicates a change in the mean composition of the aerosol load, with significantly more scattering and less absorbing aerosols than in the reference period of 2012–2019. In principle, this result could be due to distinct reasons such as the removal of absorbing aerosols or the addition of scattering aerosols. This fact suggests that although the information provided by SSA is very interesting, it cannot be interpreted alone but rather must be in combination with other aerosol parameters.

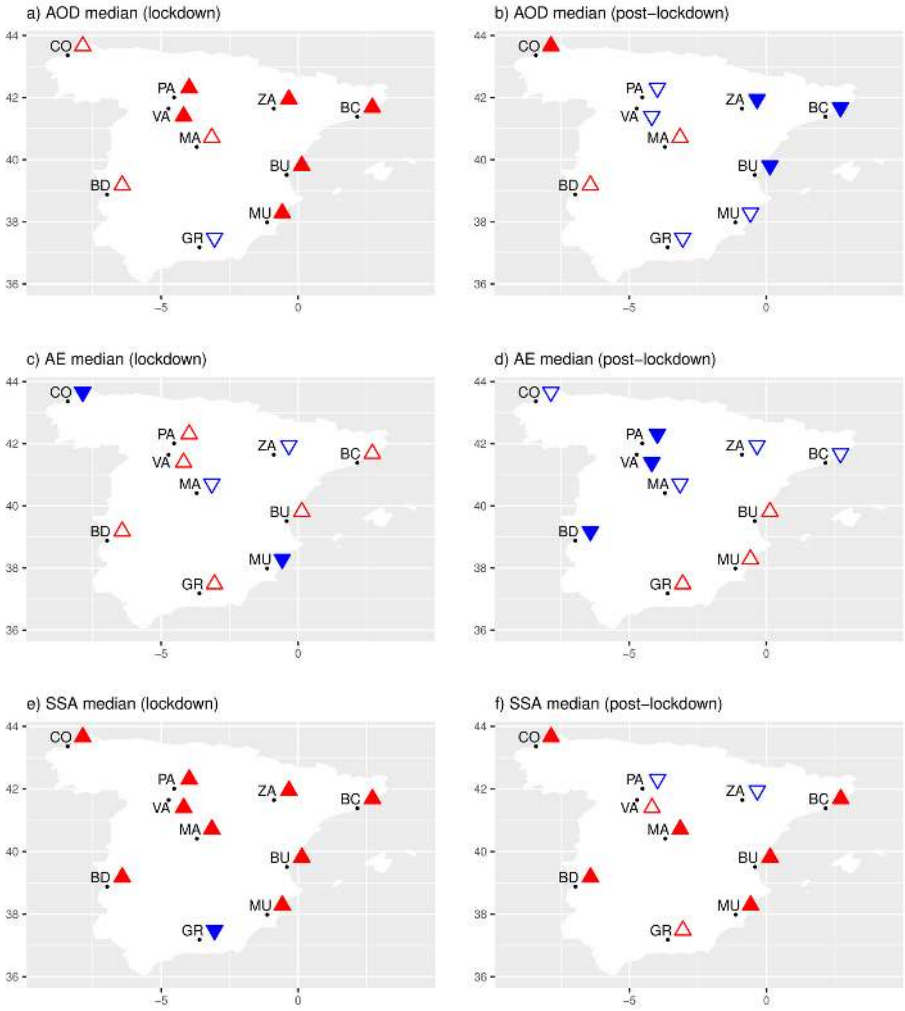

Figure 6. Sign of the change in the median of the aerosol parameters AOD, AE and SSA during the 2020 lockdown (**a**,**c**,**e**) and post-lockdown (**b**,**d**,**f**) periods compared to the reference period 2012–2019. An increase in the parameter is indicated by upward-pointing red triangles and a decrease is indicated by downward-pointing blue triangles. Closed and open symbols represent statistically significant and non-significant results, respectively, according to the central tendency test.

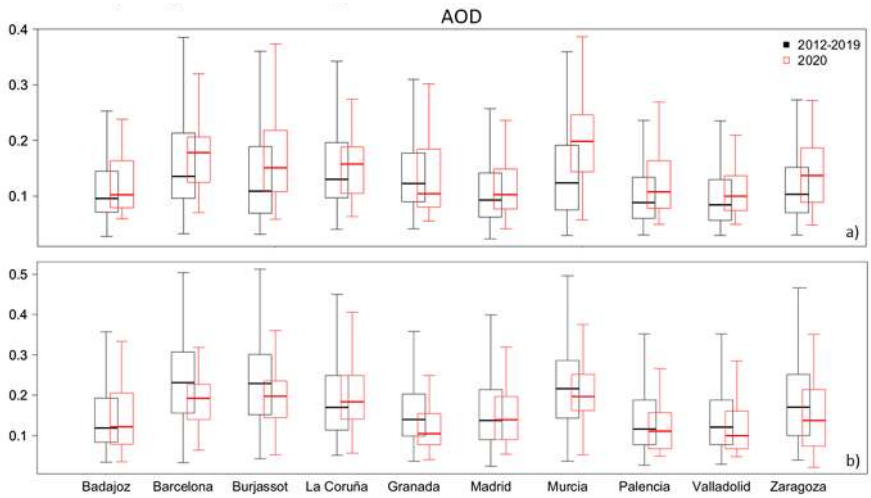

Figure 7. Box and whisker plot of AOD for each station over the 2020 lockdown (**a**) and post-lockdown (**b**) periods. The median (horizontal segment within the box), 25th and 75th percentiles (top/bottom box limits) and data within 1.5 times the interquartile range (whiskers) are shown.

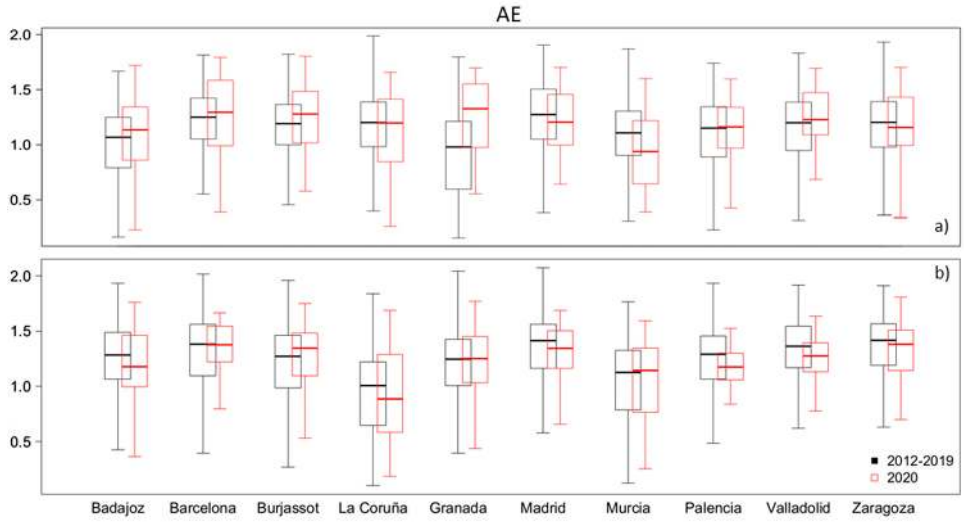

Figure 8. Box and whisker plot of AE for each station over the 2020 lockdown (**a**) and post-lockdown (**b**) periods. The median (horizontal segment within the box), 25th and 75th percentiles (top/bottom box limits) and data within 1.5 times the interquartile range (whiskers) are shown.

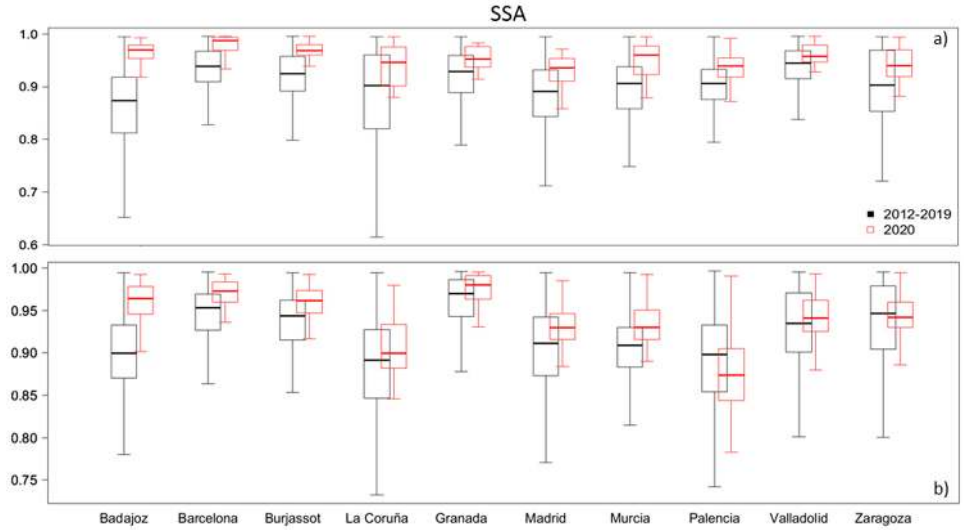

Figure 9. Box and whisker plot of SSA for each station over the 2020 lockdown (**a**) and post-lockdown (**b**) periods. The median (horizontal segment within the box), 25th and 75th percentiles (top/bottom box limits) and data within 1.5 times the interquartile range (whiskers) are shown.

4.4. Proportions Analysis

The reduction of human activity may have had a greater effect on the frequency of extreme conditions (particularly clean and turbid cases) than on the average behaviour, so the next step was to investigate changes in the lower and upper tails of the probability distribution, i.e., the low and high values of the population. The definition of low and high values requires establishing a threshold in the probability distribution. However, no general threshold can be established since the ten stations of study are located in different areas of the Iberian Peninsula and, therefore, are not equally affected by natural aerosol sources. Additionally, the cities where the stations are located show large differences in their degree of industrialisation and development of agricultural and livestock activities. Thus, while Madrid, for example, is a highly industrialised huge city with more than 7.3 million people and very heavy traffic, the city of Palencia barely reaches 80,000 inhabitants. All these reasons suggest considering relative thresholds based on the percentiles of each particular dataset. Specifically, the first and third quartiles, corresponding to the 25th and 75th percentiles of the data, respectively, were chosen. Thus, in this study, a value is considered

"low" if it is lower than the 25th percentile and is considered "high" if it is higher than the 75th percentile. With these definitions, the terms "low" and "high" acquire a local meaning since they are compared with the typical values of the dataset of the same location. Based on the distributions of the data and selected thresholds, the proportion hypothesis test determines whether the proportion of values above and below these thresholds has changed in the 2020 lockdown and post-lockdown periods compared to the same calendar days of the reference period 2012–2019.

Figures 10–12 show these changes in the proportion of cases with low and high values of AOD, AE and SSA, respectively. It is important to mention that a decrease in the proportion of days with low values of a certain parameter can be interpreted as an increase in the values of that parameter, similar to the case of an increase in the proportion of days with high values.

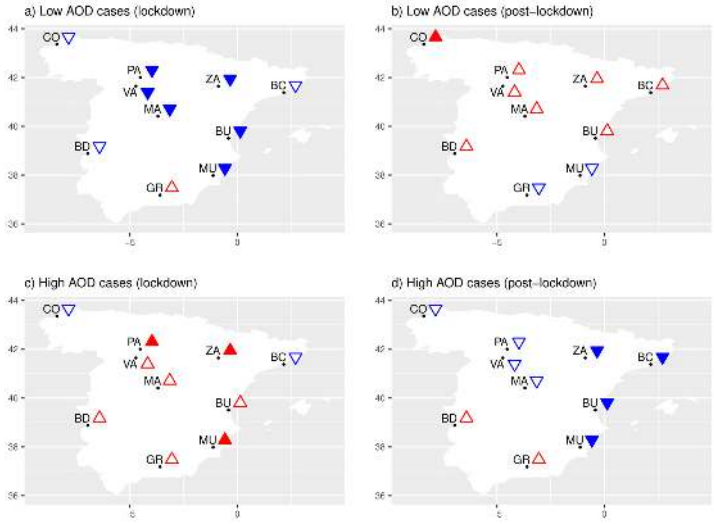

Figure 10. Sign of the change in the proportion of low/high AOD cases during the 2020 lockdown (**a**,**c**) and post-lockdown (**b**,**d**) periods compared to the 2012–2019 reference period. An increase in the proportion of cases is indicated.

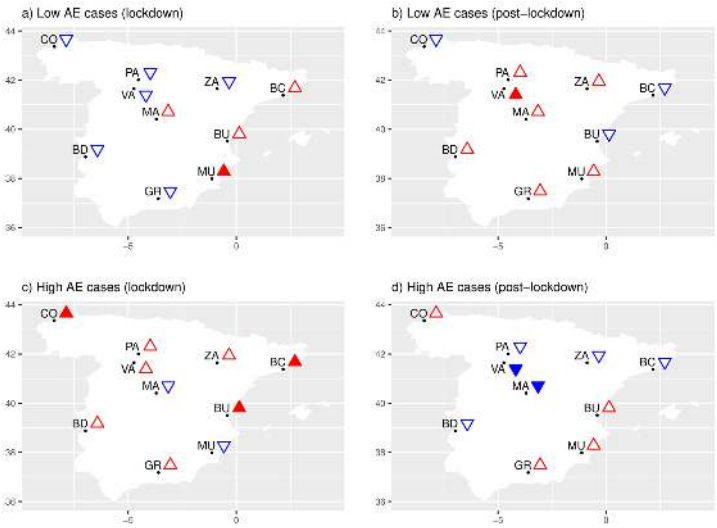

Figure 11. Sign of the change in the proportion of low/high AE cases during the 2020 lockdown (**a**,**c**) and post-lockdown (**b**,**d**) periods compared to the 2012–2019 reference period. An increase in the proportion of cases is indicated by upward-pointing red triangles and a decrease is indicated by downward-pointing blue triangles. Closed and open symbols represent statistically significant and non-significant results, respectively, according to the proportions hypothesis test.

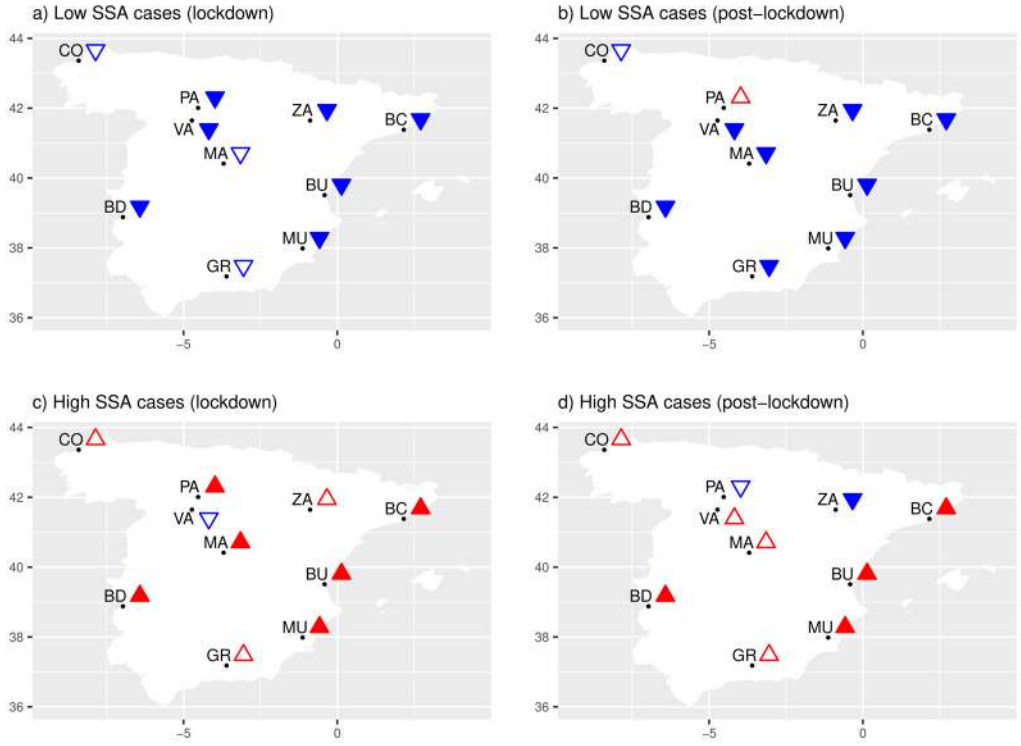

Figure 12. Sign of the change in the proportion of low/high SSA cases during the 2020 lockdown (**a**,**c**) and post-lockdown (**b**,**d**) periods compared to the 2012–2019 reference period. An increase in the proportion is indicated by upward-pointing red triangles and a decrease is indicated by downward-pointing blue triangles. Closed and open symbols represent statistically significant and non-significant results, respectively, according to the proportions hypothesis test.

4.4.1. AOD

Figure 10 shows the sign and significance of the change in AOD in the 2020 lockdown and post-lockdown periods according to the results of the proportion analysis for the clean days (low AOD values) and the turbid days (high AOD values) for the stations of study.

During the 2020 lockdown period, nine out of the ten stations experienced a decrease in the number of low AOD cases, with six of them being statistically significant (Figure 10a). A consistent trend is found for the number of high AOD cases, which increases compared to the reference period in eight stations, being statistically significant in three of them (Figure 10c). These results indicate an increase in AOD compared to the reference period in both low and high tails of the probability distribution.

This increase in AOD in Spain is in line with satellite measurements reported by other authors in the framework of large-scale studies. Thus, Acharya et al. [10] studied MODIS satellite values of AOD in south-southeast Asia, Europe and the USA during the COVID-19 pandemic and reported an increase in AOD during the period from 6 March to 30 April 2020 over Western Europe, primarily in France, Spain and Portugal. Moreover, Ibrahim et al. [11] analysed MODIS data over Europe and confirmed a 10% increase in AOD over Spain. This positive anomaly in AOD over Spain during March and April 2020 was also reported in the global studies performed by Sanap [12] and Smith et al. [13] using MODIS and CALIPSO satellites.

Several sources may have contributed to this increase in AOD such as the Saharan events detected in Madrid [53] and Barcelona [49] during this period, advecting desert dust and causing high AOD levels. These events can be clearly identified in Figure 3 as very high AOD measurements measured by several stations. Additionally, some authors bring attention to the formation of new particles. In fact, the average relative humidity over Spain during the lockdown period was very high (65%) and the average wind speed was less than 3 m/s [11]. According to Acharya et al. [10], the high moisture content combined

with low wind speed acts as a catalyst for increasing optical depth through the formation of new particles. Therefore, this high relative humidity found in Spain and combined with the light wind may have played a role in increasing AOD.

Regarding air quality, Briz-Redón et al. [41] found a decrease in PM10 measured in situ at the ground level in Spain during the lockdown, which seems to be in contrast to the detected increase in column AOD mentioned above. This result highlights the frequent discrepancies existing between the aerosol at ground level and the aerosol load of the whole atmosphere column, with the latter being sometimes driven by air masses travelling only at certain altitudes with no contribution to the near-the-ground aerosol.

On the other hand, in the 2020 post-lockdown period, most stations (eight out of the ten) showed an increase in the number of low-AOD cases (very clean days) compared to the 2012–2019 reference period, with only one of them being statistically significant (Figure 10b). This result is in line with the behaviour of the number of high-AOD cases (very turbid days), which decreased in eight stations with four of them being statistically significant (Figure 10d). These results indicate a general decrease in the AOD during the post-lockdown compared to the reference period, with more very clean days and fewer very turbid days.

4.4.2. AE

Figure 11 shows the results of applying the proportions test to the AE values for low and high-AE cases and for the 2020 lockdown and post-lockdown periods. No general tendency is found for the number of low-AE cases (large particles) in the lockdown period, with an increase at four stations and a decrease at the other six, with only one of them being statistically significant (Figure 11a). The number of high-AE cases (small particles) increases in eight of the ten stations but only three of them are statistically significant (Figure 11c). These high values during the lockdown period are characteristic of anthropogenic aerosols dominated by fine aerosols [67]. On the other hand, in the post-lockdown period, the number of stations with low AE (large particles) increases in seven stations (Figure 11b) and the number of those with high AE (small particles) decreases in six (Figure 11d), with very few significant cases from a statistical point of view. This tendency of having larger particles is in line with the expected situation caused by a reduction in anthropogenic sources, whose aerosols tend to be smaller in size than those from natural origin.

These results indicate that the column aerosol was not significantly affected immediately after the introduction of the restrictions but rather in a later period after the removal of the most restrictive measures in most European countries. Similar behaviour was observed at several sites in south-eastern Italy [45] and in Paris [46]. This fact could be due to the fact that most atmospheric particles are not directly emitted into the atmosphere, as is the case for gaseous pollutants [68,69]. Instead, atmospheric particles can also be formed by coagulation, mixing and secondary processes, which, in turn, depend on the residence time of the particles in the atmosphere.

4.4.3. SSA

Figure 12 shows the results of applying the proportion hypothesis test to the SSA values at each location for the 2020 lockdown and post-lockdown periods. A general and significant increase in SSA is found during both the 2020 lockdown and post-lockdown periods compared to the 2012–2019 reference period. In both the lockdown and post-lockdown periods, the proportion analysis shows a notable decrease in the number of low-SSA cases (more absorbing aerosols) and also a marked increase in the number of high-SSA cases (more scattering aerosols). Thus, during the lockdown, all the stations showed a decrease in the number of low-SSA cases and almost all of them also showed an increase in the number of high-SSA cases, with seven and six stations that have statistically significant results, respectively. Similarly, during the post-lockdown, the number of low-SSA cases decreased in nine stations (being statistically significant in eight of them), and the number of high-SSA cases increased in eight stations (being significant in five of them).

Therefore, it can be concluded that aerosols were more scattering and less absorbing in the 2020 lockdown and post-lockdown periods than those on the same calendar days in the 2012–2019 period. This finding is also reported by Barragán et al. [53] for the Madrid station.

Among the three aerosol parameters studied, SSA proved to be the variable most sensitive to changes in the 2020 lockdown and post-lockdown periods compared to the reference period.

5. Discussion

The preliminary examination of Figures 3–5 and 7–9 and the general analysis based on ANOVA evidenced the existence of unusual values of some aerosol parameters during the 2020 lockdown and post-lockdown compared to the values measured during the same calendar days during the 2012–2019 reference period. These analyses were followed by individual tests conducted over the three quartiles Q1, Q2 (the median) and Q3 for each station and each aerosol parameter. The results revealed differences between stations, emphasising the difficulty of discerning the effect of a specific contribution on the whole aerosol column. It is important to note that the column aerosol load over a given location is generally the very complex result of the mixing of aerosols of different types coming from several sources at various spatial scales. In this mixing, local factors such as the surrounding orography also play an important role. Furthermore, these mixing changes with time, as predominant factors vary. Finally, this mixing changes between sites, as they differ both in terms of relevant local factors and in the exposure of each site to air masses from other regions.

In this complex framework where the effect of lockdown could be masked by the local variability specific to each site, the joint analysis of the first (Q1), second (Q2, i.e., median) and third quartiles constitutes a means of checking the reliability of the results. Thus, the results are reaffirmed if the three quartiles show the same tendency (all increase or all decrease). Conversely, the confidence in the results decreases if, for example, the first and third quartiles have a certain tendency but the second quartile shows the opposite tendency. In this sense, the statistically significant results obtained in this study for the three quartiles show consistent tendencies in 92% of the cases, with the agreement being reduced to 84% when the results of the tests that were not statistically significant are included. These percentages give confidence in the test results and in the conclusions that can be drawn.

In order to find groups of stations showing a common behaviour, the changes in the three aerosol parameters that occurred during the 2020 lockdown and post-lockdown periods (Figures 6 and 10–12) were examined as a function of the geographical location of the stations, their proximity to the sea, their influence by the Atlantic or Mediterranean seas, the size of the city and the urban or rural surroundings of the station. In principle, these factors could lead to a certain degree of consistency between similar sites. Thus, for example, the proximity to Africa increases the possibility of desert dust intrusions, being close to the coast favours air renewal by the daily sea breeze, and an urban or rural environment provides a specific aerosol load.

The joint analysis of stations and quartiles shows a general increase in AOD in the 2020 lockdown and a decrease in the 2020 post-lockdown compared to the same calendar days of the 2012–2019 reference period. This AOD pattern of variation is followed by all stations except A Coruña and Granada, which show particular behaviours likely driven by the large exposure of A Coruña to Atlantic winds, and the relevant role of orography in the case of Granada. Regarding AE, no general behaviour during the lockdown and the post-lockdown is found, and most of the test results are nonsignificant from a statistical point of view. In contrast, SSA shows the most significant agreement between stations and quartiles, with nearly all of the test results being significant and indicating the increase in SSA during both the lockdown and the post-lockdown periods.

Among the eight stations that behave consistently with respect to the variation in SSA and AOD, Palencia and Valladolid show the greatest similarity and the same tendency in all tests. This similarity was to be expected since they are only 39 km apart. In addition

to these two general behaviours, no other common pattern is found. Thus, neither the more urban sites, such as Barcelona and Madrid, nor the more rural sites, such as Badajoz and Palencia, show a greater similarity than with other stations. No particularly similar behaviour is found for coastal versus inland sites either.

In principle, the increase found in SSA can be due to two different causes: the removal of absorbing aerosols or the addition of predominantly scattering aerosols. This fact suggests that, although the information provided by SSA is very interesting, it must be interpreted in combination with other aerosol parameters. Thus, when the SSA is analysed together with the AOD, two different situations appear: (1) the lockdown period, with high values of AOD and SSA, and (2) the post-lockdown period, with low values of AOD and high values of SSA.

The high values of AOD during the 2020 lockdown are in agreement with the catalogue of aerosol events reported by the Consejo Superior de Investigaciones Científicas [70]. This report states that the number of days affected by desert dust intrusions coming from the Sahara was markedly high during the 2020 lockdown, with a surplus of 49% above the median value obtained during the period of 2012–2019 for the same calendar days. Thus, the high values of AOD and SSA during the lockdown are likely due to desert dust intrusions that bring high loadings of scattering aerosols.

In contrast, the number of days with desert dust events during the post-lockdown is very similar to the typical values registered during the period of 2012–2019 for the same calendar days, with only 3% above the median frequency [70]. This fact, combined with the low values of AOD and the high values of SSA, indicates the depletion of absorbing aerosols. This result is in line with the reduction in traffic and industry activities, which are responsible for most of the black-carbon emissions.

6. Conclusions

This study takes advantage of the unique situation offered by the 2020 COVID-19 lockdown to investigate the effect of reduced road traffic and human activities on column aerosols. It aims to improve our understanding of the contribution of anthropogenic sources to the total aerosol load.

In order to meet that aim, high-quality measurements provided by the AERONET network have been used. In contrast to most previous papers, the present study focuses on column aerosols, i.e., the aerosol load integrated along the entire atmospheric column. This column aerosol is a key factor in understanding the radiation balance and climate change and shows a specific behaviour different from that of the aerosol near the ground measured by in situ stations.

The study proposes a comprehensive methodology based on three statistical tests that aim to detect footprints of the COVID-19 lockdown in different characteristics of the dataset. Thus, in addition to testing for changes in the median values of the aerosol parameters, the increase or decrease in the number of days with low or high values of the parameters is examined. This proposal provides suitable methodologies to detect subtle changes in such a complex mixture of anthropogenic and natural sources. The tests have proven to be effective in detecting changes in the aerosol parameters. The main results indicate that AOD increased in the lockdown period and decreased in the post-lockdown period. This result is in line with Barragán et al. [53] for the particular case of Madrid and with satellite studies that found an increase in AOD in the southwest of Europe during the 2020 lockdown [10–13].

This increase in AOD during the lockdown period seems to be in contrast to the PM decrease reported by other authors for different locations in Spain [34,41,49–52]. This discrepancy emphasises the differences between the behaviour shown by the aerosol near the ground measured by in situ techniques and the column aerosol, which is often driven by advected air masses travelling long distances.

While AE shows no general trend, SSA shows a general and significant increase at most sites during the 2020 lockdown and post-lockdown periods. This means that the ratio

of absorbing aerosols to scattering aerosols decreased. The combined analysis of the AOD and SSA indicates that, while the high SSA values during the 2020 lockdown were likely caused by desert dust intrusions, the high values of SSA post-lockdown were also likely related to the depletion of absorbing aerosol due to the reduction in traffic and industry activities. This conclusion is also in line with the higher frequency of desert dust events during the lockdown as reported by [70].

These results indicate that SSA is the most sensitive parameter to the changes in the contribution of anthropogenic sources that occurred during the 2020 lockdown and post-lockdown periods and is, therefore, relevant for other studies dealing with the detection of the COVID-19 lockdown footprints in the column aerosol. Thus, SSA has been shown to provide very interesting information that, in combination with AOD, helps to discriminate between different aerosol sources. This finding is particularly innovative since many classifications of aerosols into different types are based exclusively on AOD and AE [71–74].

This study contributes to a better knowledge of the changes in the column aerosol due to the 2020 COVID-19 lockdown as measured from surface stations, which has been poorly studied in comparison to those based on satellite or in situ data. However, it should be noted that it focuses on the detection of footprints of the 2020 COVID-19 lockdown on the column-integrated aerosol parameters and does not quantify its specific contribution, as other factors such as meteorology and the regional and long-term transport of aerosols may also have their own contributions.

Author Contributions: Conceptualization, A.S. and M.Á.O.; methodology, B.M. and A.S.; software, B.M.; validation, M.Á.O.; formal analysis, B.M.; investigation, B.M. and M.Á.O.; resources, A.S. and M.Á.O.; data curation, B.M. and M.Á.O.; writing—original draft preparation, M.Á.O. and A.S.; writing—review and editing, A.S.; visualisation, A.S. and B.M.; supervision, M.Á.O. and A.S.; project administration, A.S. and M.Á.O.; funding acquisition, M.Á.O. and A.S. All authors have read and agreed to the published version of the manuscript.

Funding: This work was supported through the Grant TED2021-130532A-I00 funded by MCIN/AEI/10.13039/501100011033 and by the "European Union NextGenerationEU/PRTR".

Data Availability Statement: Publicly available datasets were analysed in this study. These data can be found on the AERONET website: https://aeronet.gsfc.nasa.gov/ (accessed on 10 March 2023).

Acknowledgments: Thanks are due to AERONET/PHOTONS and RIMA networks for the scientific and technical support. CIMEL calibration was performed at the AERONET-EUROPE GOA calibration center, supported by ACTRIS under agreement no. 871115 granted by the European Union. We thank Manuel Molina and Jacinto R. Martín from Departamento de Matemáticas, Universidad de Extremadura, for their advice on the statistical tests. The authors gratefully acknowledge the Ministerio para la Transición Ecológica y Reto Demográfico and the Consejo Superior de Investigaciones Científicas (CSIC) for the provision of the catalogue of aerosol events used in this publication.

Conflicts of Interest: The authors declare no conflict of interest.

References

1. Eyring, V.; Gillett, N.P.; Achuta Rao, K.M.; Barimalala, R.; Barreiro Parrillo, M.; Bellouin, N.; Cassou, C.; Durack, P.J.; Kosaka, Y.; McGregor, S.; et al. Human Influence on the Climate System. In *Climate Change 2021: The Physical Science Basis*; Contribution of Working Group I to the Sixth Assessment Report of the Intergovernmental Panel on Climate Change; Masson-Delmotte, V.P., Zhai, A., Pirani, S.L., Connors, C., Péan, S., Berger, N., Caud, Y., Chen, L., Goldfarb, M.I., Gomis, M., et al., Eds.; Cambridge University Press: Cambridge, UK; New York, NY, USA, 2021; pp. 423–552. [CrossRef]
2. IPCC. Climate Change 2022: Impacts, Adaptation, and Vulnerability. In *Contribution of Working Group II to the Sixth Assessment Report of the Intergovernmental Panel on Climate Change*; Pörtner, H.-O., Roberts, D.C., Tignor, M., Poloczanska, E.S., Mintenbeck, K., Alegría, A., Craig, M., Langsdorf, S., Löschke, S., Möller, V., et al., Eds.; Cambridge University Press: Cambridge, UK; New York, NY, USA, 2022; 3056p. [CrossRef]
3. Myhre, G.; Myhre, C.E.L.; Samset, B.H.; Storelvmo, T. Aerosols and their Relation to Global Climate and Climate Sensitivity. *Nat. Educ. Knowl.* **2013**, *4*, 7.
4. Chauhan, A.; Singh, R.P. Decline in PM2.5 concentrations over major cities around the world associated with COVID-19. *Environ. Res.* **2020**, *187*, 109634. [CrossRef] [PubMed]

5. Venter, Z.S.; Aunan, K.; Chowdhury, S.; Lelieveld, J. Air pollution declines during COVID-19 lockdowns mitigate the global health burden. *Environ. Res.* **2020**, *192*, 110403. [CrossRef] [PubMed]
6. Habibi, H.; Awal, R.; Fares, A.; Ghahremannejad, M. COVID-19 and the Improvement of the Global Air Quality: The Bright Side of a Pandemic. *Atmosphere* **2020**, *11*, 1279. [CrossRef]
7. He, C.; Hong, S.; Zhang, L.; Mu, H.; Xin, A.; Zhou, Y.; Liu, J.; Liu, N.; Su, Y.; Tian, Y.; et al. Global, continental, and national variation in PM2.5, O_3, and NO_2 concentrations during the early 2020 COVID-19 lockdown. *Atmos. Pollut. Res.* **2021**, *12*, 136–145. [CrossRef]
8. Kumari, P.; Toshniwal, D. Impact of lockdown on air quality over major cities across the globe during COVID-19 pandemic. *Urban Clim.* **2020**, *34*, 100719. [CrossRef]
9. Rodríguez-Urrego, D.; Rodríguez-Urrego, L. Air quality during the COVID-19: PM2.5 analysis in the 50 most polluted capital cities in the world. *Environ. Pollut.* **2020**, *266*, 115042. [CrossRef]
10. Acharya, P.; Barik, G.; Gayen, B.K.; Bar, S.; Maiti, A.; Sarkar, A.; Ghosh, S.; De, S.K.; Sreekesh, S. Revisiting the levels of Aerosol Optical Depth in south-southeast Asia, Europe and USA amid the COVID-19 pandemic using satellite observations. *Environ. Res.* **2021**, *193*, 110514. [CrossRef]
11. Ibrahim, S.; Landa, M.; Pešek, O.; Pavelka, K.; Halounova, L. Space-Time Machine Learning Models to Analyze COVID-19 Pandemic Lockdown Effects on Aerosol Optical Depth over Europe. *Remote Sens.* **2021**, *13*, 3027. [CrossRef]
12. Sanap, S.D. Global and regional variations in aerosol loading during COVID-19 imposed lockdown. *Atmos. Environ.* **2021**, *246*, 118132. [CrossRef]
13. Smith, S.E.; Ting, M.; Wu, Y.; Zheng, C. Beyond the lockdowns: Satellite observations of aerosol optical depth through 2020, the first year of the COVID-19 pandemic. *Environ. Res. Lett.* **2022**, *7*, 17. [CrossRef]
14. Zheng, H.; Kong, S.; Chen, N.; Yan, Y.; Liu, D.; Zhu, B.; Xu, K.; Cao, W.; Ding, Q.; Lan, B.; et al. Significant changes in the chemical compositions and sources of PM2.5 in Wuhan since the city lockdown as COVID-19. *Sci. Total Environ.* **2020**, *739*, 140000. [CrossRef] [PubMed]
15. Tian, J.; Wang, Q.; Zhang, Y.; Yan, M.; Liu, H.; Zhang, N.; Ran, W.; Cao, J. Impacts of primary emissions and secondary aerosol formation on air pollution in an urban area of China during the COVID-19 lockdown. *Environ. Int.* **2021**, *150*, 106426. [CrossRef] [PubMed]
16. Chen, H.; Huo, J.; Fu, Q.; Duan, Y.; Xiao, H.; Chen, J. Impact of quarantine measures on chemical compositions of PM2.5 during the COVID-19 epidemic in Shanghai, China. *Sci. Total Environ.* **2020**, *743*, 140758. [CrossRef]
17. Huang, X.; Ding, A.; Gao, J.; Zheng, B.; Zhou, D.; Qi, X.; Tang, R.; Wang, J.; Ren, C.; Nie, W.; et al. Enhanced secondary pollution offset reduction of primary emissions during COVID-19 lockdown in China. *Natl. Sci. Rev.* **2021**, *8*, nwaa137. [CrossRef] [PubMed]
18. Chen, Z.; Hao, X.; Zhang, X.; Chen, F. Have Traffic Restrictions Improved Air Quality? A Shock from COVID-19. *J. Clean. Prod.* **2021**, *279*, 123622. [CrossRef]
19. Le, T.; Wang, Y.; Liu, L.; Yang, J.; Yung, Y.L.; Li, G.; Seinfeld, J.H. Unexpected air pollution with marked emission reductions during the COVID-19 outbreak in China. *Science* **2020**, *369*, 702–706. [CrossRef]
20. Mahato, S.; Pal, S.; Ghosh, K.G. Effect of lockdown amid COVID-19 pandemic on air quality of the megacity Delhi, India. *Sci. Total Environ.* **2020**, *730*, 086. [CrossRef]
21. Kerimray, A.; Baimatova, N.; Ibragimova, O.P.; Bukenov, B.; Kenessov, B.; Plotitsyn, P.; Karaca, F. Assessing air quality changes in large cities during COVID-19 lockdowns: The impacts of traffic-free urban conditions in Almaty, Kazakhstan. *Sci. Total Environ.* **2020**, *730*, 139179. [CrossRef]
22. Zoran, M.A.; Savastru, R.S.; Savastru, D.M.; Tautan, M.N. Peculiar weather patterns effects on air pollution and COVID-19 spread in Tokyo metropolis. *Environ. Res.* **2023**, *228*, 115907. [CrossRef]
23. Santoso, M.; Hopke, P.K.; Permadi, D.A.; Damastuti, E.; Lestiani, D.D.; Kurniawati, S.; Khoerotunnisya, D.; Sukir, S.K. Multiple Air Quality Monitoring Evidence of the Impacts of Large-scale Social Restrictions during the COVID-19 Pandemic in Jakarta, Indonesia. *Aerosol Air Qual. Res.* **2021**, *21*, 200645. [CrossRef]
24. Wetchayont, P.; Hayasaka, T.; Khatri, P. Air Quality Improvement during COVID-19 Lockdown in Bangkok Metropolitan, Thailand: Effect of the Long-range Transport of Air Pollutants. *Aerosol Air Qual. Res.* **2021**, *21*, 200662. [CrossRef]
25. Shukla, N.; Sharma, G.K.; Baruah, P.; Shukla, V.K.; Gargava, P. Impact of Shutdown due to COVID-19 Pandemic on Aerosol Characteristics in Kanpur, India. *J. Health Pollut.* **2020**, *10*, 201201. [CrossRef] [PubMed]
26. Shen, L.; Zhao, T.; Wang, H.; Liu, J.; Bai, Y.; Kong, S.; Zheng, H.; Zhu, Y.; Shu, Z. Importance of meteorology in air pollution events during the city lockdown for COVID-19 in Hubei Province, Central China. *Sci. Total Environ.* **2021**, *754*, 142227. [CrossRef]
27. Adams, M.D. Air Pollution in Ontario, Canada during the COVID-19 State of Emergency. *Sci. Total Environ.* **2020**, *742*, 140516. [CrossRef] [PubMed]
28. Chen, L.W.A.; Chien, L.C.; Li, Y.; Lin, G. Nonuniform Impacts of COVID-19 Lockdown on Air Quality over the United States. *Sci. Total Environ.* **2020**, *745*, 141105. [CrossRef] [PubMed]
29. Kutralam-Muniasamy, G.; Pérez-Guevara, F.; Roy, P.D.; Elizalde-Martínez, I.; Shruti, V.C. Impacts of the COVID-19 lockdown on air quality and its association with human mortality trends in megapolis Mexico City. *Air Qual. Atmos. Health* **2021**, *14*, 553–562. [CrossRef]

30. Dantas, G.; Siciliano, B.; França, B.; da Silva, C.M.; Arbilla, G. The impact of COVID-19 partial lockdown on the air quality of the city of Rio de Janeiro, Brazil. *Sci. Total Environ.* **2020**, *729*, 139085. [CrossRef]
31. Nakada, L.Y.K.; Urban, R.C. COVID-19 pandemic: Impacts on the air quality during the partial lockdown in São Paulo state, Brazil. *Sci. Total Environ.* **2020**, *730*, 139087. [CrossRef]
32. Bolaño-Ortiz, T.R.; Pascual-Flores, R.M.; Puliafito, S.E.; Camargo-Caicedo, Y.; Berná-Peña, L.L.; Ruggeri, M.F.; López-Noreña, A.I.; Tames, M.F.; Cereceda-Balic, F. Spread of COVID-19, Meteorological Conditions and Air Quality in the City of Buenos Aires, Argentina: Two Facets Observed during Its Pandemic Lockdown. *Atmosphere* **2020**, *11*, 1045. [CrossRef]
33. Duc, H.; Salter, D.; Azzi, M.; Jiang, N.; Warren, L.; Watt, S.; Riley, M.; White, S.; Trieu, T.; Tzu-Chi Chang, L.; et al. The Effect of Lockdown Period during the COVID-19 Pandemic on Air Quality in Sydney Region, Australia. *Int. J. Environ. Res. Public Health* **2021**, *18*, 3528. [CrossRef]
34. Skirienė, A.F.; Stasiškienė, Ž. COVID-19 and Air Pollution: Measuring Pandemic Impact to Air Quality in five European Countries. *Atmosphere* **2021**, *12*, 290. [CrossRef]
35. Jephcote, C.; Hansell, A.L.; Adams, K.; Gulliver, J. Changes in air quality during COVID-19 'lockdown' in the United Kingdom. *Environ. Pollut.* **2021**, *272*, 116011. [CrossRef]
36. Cao, X.; Liu, X.; Hadiatullah, H.; Xu, Y.; Zhang, X.; Cyrys, J.; Zimmermann, R.; Adam, T. Investigation of COVID-19-related lockdowns on the air pollution changes in augsburg in 2020, Germany. *Atmos. Pollut. Res.* **2022**, *13*, 101536. [CrossRef]
37. Rogulski, M.; Badyda, A. Air Pollution Observations in Selected Locations in Poland during the Lockdown Related to COVID-19. *Atmosphere* **2021**, *12*, 806. [CrossRef]
38. Donzelli, G.; Cioni, L.; Cancellieri, M.; Llopis Morales, A.; Morales Suárez-Varela, M.M. The Effect of the COVID-19 Lockdown on Air Quality in Three Italian Medium-Sized Cities. *Atmosphere* **2020**, *11*, 1118. [CrossRef]
39. Sbai, S.E.; Mejjad, N.; Norelyaqine, A.; Bentayeb, F. Air quality change during the COVID-19 pandemic lockdown over the Auvergne-Rhône-Alpes region, France. *Air Qual. Atmos. Health* **2021**, *14*, 617–628. [CrossRef]
40. Dahech, S.; Abdmouleh, M.A.; Lagmiri, S. Spatiotemporal Variation of Air Quality (PM and NO2) in Southern Paris during COVID-19 Lockdown Periods. *Atmosphere* **2022**, *13*, 289. [CrossRef]
41. Briz-Redón, A.; Belenguer-Sapiña, C.; Serrano-Aroca, A. Changes in air pollution during COVID-19 lockdown in Spain: A multi-city study. *J. Environ. Sci.* **2020**, *101*, 16–26. [CrossRef]
42. Querol, X.; Massagué, J.; Alastuey, A.; Moreno, T.; Gangoiti, G.; Mantilla, E.; Diéguez, J.J.; Escudero, M.; Monfort, E.; García-Pando, C.P.; et al. Lessons from the COVID-19 air pollution decrease in Spain: Now what? *Sci. Total Environ.* **2021**, *779*, 146380. [CrossRef]
43. Gama, C.; Relvas, H.; Lopes, M.; Monteiro, A. The impact of COVID-19 on air quality levels in Portugal: A way to assess traffic contribution. *Environ. Res.* **2021**, *193*, 110515. [CrossRef] [PubMed]
44. Gamelas, C.; Abecasis, L.; Canha, N.; Almeida, S.M. The Impact of COVID-19 Confinement Measures on the Air Quality in an Urban-Industrial Area of Portugal. *Atmosphere* **2021**, *12*, 1097. [CrossRef]
45. Romano, S.; Catanzaro, V.; Paladini, F. Impacts of the COVID-19 Lockdown Measures on the 2020 Columnar and Surface Air Pollution Parameters over South-Eastern Italy. *Atmosphere* **2021**, *12*, 1366. [CrossRef]
46. Piazzola, J.; Bruch, W.; Desnues, C.; Parent, P.; Yohia, C.; Canepa, E. Influence of Meteorological Conditions and Aerosol Properties on the COVID-19 Contamination of the Population in Coastal and Continental Areas in France: Study of Offshore and Onshore Winds. *Atmosphere* **2021**, *12*, 523. [CrossRef]
47. Filonchyk, M.; Hurynovich, V.; Yan, H. Impact of COVID-19 lockdown on air quality in the Poland, Eastern Europe. *Environ. Res.* **2021**, *198*, 110454. [CrossRef]
48. Sannino, A.; D'Emilio, M.; Castellano, P.; Amoruso, S.; Boselli, A. Analysis of Air Quality during the COVID-19 Pandemic Lockdown in Naples (Italy). *Aerosol Air Qual. Res.* **2021**, *21*, 200381. [CrossRef]
49. Tobías, A.; Carnerero, C.; Reche, C.; Massagué, J.; Via, M.; Minguillón, M.C.; Alastuey, A.; Querol, X. Changes in air quality during the lockdown in Barcelona (Spain) one month into the SARS-CoV-2 epidemic. *Sci. Total Environ.* **2020**, *726*, 138540. [CrossRef]
50. Betancourt-Odio, M.A.; Martínez-de-Ibarreta, C.; Budría-Rodríguez, S.; Wirth, E. Local analysis of air quality changes in the community of Madrid before and during the COVID-19 induced lockdown. *Atmosphere* **2021**, *12*, 659. [CrossRef]
51. Donzelli, G.; Cioni, L.; Cancellieri, M.; Llopis-Morales, A.; Morales-Suárez-Varela, M. Relations between air quality and COVID-19 lockdown measures in Valencia, Spain. *Int. J. Environ. Res. Public Health* **2021**, *18*, 2296. [CrossRef]
52. Wirth, E.; Betancourt-Odio, M.A.; Cabeza-García, M.; Zapatero-González, A. Footprints of COVID-19 on Pollution in Southern Spain. *Atmosphere* **2022**, *13*, 1928. [CrossRef]
53. Barragán, R.; Molero, F.; Granados-Muñoz, M.J.; Salvador, P.; Pujadas, M.; Artiñano, B. Feasibility of Ceilometers Data to Estimate Radiative Forcing Values: Application to Different Conditions around the COVID-19 Lockdown Period. *Remote Sens.* **2020**, *12*, 3699. [CrossRef]
54. Mitjà, O.; Arenas, A.; Rodó, X.; Tobías, A.; Brew, J.; Benlloch, J.M. Experts' request to the Spanish Government: Move Spain towards complete lockdown. *Lancet* **2020**, *395*, 1193–1194. [CrossRef]
55. Holben, B.; Eck, T.F.; Slutsker, I.; Tanre, D.; Buis, J.; Setzer, K.; Vermote, E.; Reagan, J.; Kaufman, Y.; Nakajima, T.; et al. AERONET—A federated instrument network and data archive for aerosol characterization. *Remote Sens. Environ.* **1998**, *66*, 1–16. [CrossRef]
56. Schuster, G.L.; Dubovik, O.; Holben, B.N. Ångström exponent and bimodal aerosol size distributions. *J. Geophys. Res.* **2006**, *111*, D07207. [CrossRef]

57. Dubovik, O.; Smirnov, A.; Holben, B.N.; King, M.D.; Kaufman, Y.J.; Eck, T.F.; Slutsker, I. Accuracy assessments of aerosol optical properties retrieved from Aerosol Robotic Network (AERONET) Sun and sky radiance measurements. *J. Geophys. Res.* **2000**, *105*, 9791–9806. [CrossRef]
58. Jonhson, D.H. The Insignificance of Statistical Significance Testing. *J. Wildl. Manag.* **1999**, *3*, 763–772. [CrossRef]
59. Lakens, D. The practical alternative to the p value is the correctly used p value. *Perspect Psychol Sci.* **2021**, *16*, 639–648. [CrossRef]
60. Fricker, R.D., Jr.; Burke, K.; Han, X.; Woodall, W.H. Assessing the Statistical Analyses Used in Basic and Applied Social Psychology after Their p-Value Ban. *Am. Stat.* **2019**, *73*, 374–384. [CrossRef]
61. Girden, E.R. *ANOVA: Repeated Measures*; Sage: Thousand Oaks, CA, USA, 1992.
62. Kaufmann, J.; Schering, A.G. Analysis of variance (ANOVA). In *Wiley Encyclopedia of Clinical Trials*; D'Agostino, R., Massaro, J., Sullivan, L., Eds.; Wiley: Hoboken, NJ, USA, 2007. [CrossRef]
63. Black, G.; Ard, D.; Smith, J.; Schibik, T. The impact of the Weibull distribution on the performance of the single-factor ANOVA model. *Int. J. Ind. Eng. Comput.* **2010**, *1*, 185–198. [CrossRef]
64. Lantz, B. The impact of sample non-normality on ANOVA and alternative methods. *Br. J. Math. Stat. Psychol.* **2013**, *66*, 224–244. [CrossRef]
65. Schmider, E.; Ziegler, M.; Danay, E.; Beyer, L.; Bühner, M. Is it really robust? Reinvestigating the robustness of ANOVA against violations of the normal distribution assumption. *Methodology* **2010**, *6*, 147–151. [CrossRef]
66. Blanca Mena, M.J.; Alarcón Postigo, R.; Arnau Gras, J.; Bono Cabré, R.; Bendayan, R. Non-normal data: Is ANOVA still a valid option? *Psicothema* **2017**, *29*, 552–557.
67. Kleidman, R.G.; O'Neill, N.T.; Remer, L.A.; Kaufman, Y.J.; Eck, T.F.; Tanre, D.; Dubovik, O.; Holben, B.N. Comparison of Moderate Resolution Imaging Spectroradiometer (MODIS) and Aerosol Robotic Network (AERONET) remote-sensing retrieval of aerosol fine mode fraction over ocean. *J. Geophys. Res.* **2005**, *110*, D22205. [CrossRef]
68. Lonati, G.; Riva, F. Regional scale impact of the COVID-19 Lockdown on Air Quality: Gaseous Pollutants in the Po Valley, Northern Italy. *Atmosphere* **2021**, *12*, 264. [CrossRef]
69. Marinello, S.; Lolli, F.; Gamberini, R. The Impact of the COVID-19 Emergency on Local Vehicular Traffic and Its Consequences for the Environment: The Case of the City of Reggio Emilia (Italy). *Sustainability* **2021**, *13*, 118. [CrossRef]
70. Ministerio Para la Transición Ecológica y el Reto Demográfico (MITECO). Episodios naturales de Partículas. *African Dust Alert System.* Available online: https://www.miteco.gob.es/es/calidad-y-evaluacion-ambiental/temas/atmosfera-y-calidad-del-aire/calidad-delaire/evaluacion-datos/fuentes-naturales/default.aspx (accessed on 31 March 2023).
71. Elias, T.; Silva, A.; Belo, N.; Pereira, S.; Formenti, P.; Helas, G.; Wagner, F. Aerosol extinction in a remote continental region of the Iberian Peninsula during summer. *J. Geophys. Res.* **2006**, *111*, 1–20. [CrossRef]
72. Otero, L.; Ristori, P.; Holben, B.; Quel, E. Espesor óptico de aerosoles durante el año 2002 para diez estaciones pertenecientes a la red AERONET—NASA. *Opt. Pura Apl.* **2006**, *39*, 355–364.
73. Kaskaoutis, D.; Kambezidis, H.; Hatzianastassiou, N.; Kosmopoulos, P.; Badarinath, K. Aerosol climatology: On the discrimination of aerosol types over four Aeronet sites. Atmos. *Chem. Phys. Discuss.* **2007**, *7*, 6357–6411.
74. Toledano, C.; Cachorro, V.; Berjón, A.; de Frutos, A.; Sorribas, M.; de la Morena, B.; Goloub, P. Aerosol optical depth and Ångström exponent climatology at El Arenosillo AERONET site (Huelva, Spain). *Q. J. R. Meteorol. Soc.* **2007**, *133*, 795–807. [CrossRef]